The Aeronautical Journal (2023), **127**, pp. 818–830
doi:10.1017/aer.2022.90

REGULAR PAPER

A fuzzy model to predict the mechanical characteristics of friction stir welded joints of aluminum alloy AA2014-T6

S.K. Ashok[1] and S. Ponni alias sathya[2,*]

[1]Automobile Engineering, Dr. Mahalingam College of Engineering & Technology, Pollachi, Tamil Nadu, India and
[2]Information Technology, Dr. Mahalingam College of Engineering & Technology, Pollachi, Tamil Nadu, India
*Correspondence author. Email: sathyaashok2007@gmail.com

Received: 5 May 2022; **Revised:** 30 September 2022; **Accepted:** 10 October 2022

Keywords: friction stirwelding; fuzzy logic; aluminium alloy AA2014-T6; micro hardness; tensile strength

Abstract

Friction stir welding is a prominent technique for making defect-free joints of aluminum alloys. The aluminum alloy AA2014-T6 finds wide applications in aerospace, naval and automotive applications. This paper attempts to predict the tensile strength and hardness characteristics of friction stir welded aluminum alloy AA2014-T6 by a fuzzy logic model. Friction stir welding was carried out by varying tool rotational speed (700, 1,000 and 1,400rpm), welding speed (20, 35, 50mm/min) and axial force (10, 12, 14kN) at three levels. The tensile strength and hardness characteristics of the welded specimens were obtained from the experiments conducted as per Taguchi's L_{27} orthogonal array. A Mamdani-type fuzzy logic model was developed to predict the tensile strength and nugget hardness characteristics of the FSW joints. The fuzzy model was evaluated by comparing the results of confirmation experiments with that of the results predicted by the model. The confirmation experiments were conducted with a new set of parameters other than the ones used for building the model. The fuzzy model exhibits marginal variations of 2.53% for tensile strength and 2.42% for weld nugget hardness compared to the results of the conformation experiments.

Nomenclature

FSW	Friction Stir Welding
MF	Membership Function
RMSE	Root Mean Square Error
NDT	Non-Destructive Testing
TRS	Tool Rotational Speed
WS	Welding Speed
AF	Axial Force
FIS	Fuzzy Inference Systems
TS	Tensile Strength
NH	Nugget Hardness
TMAZ	Thermo Mechanically Affected Zone
HAZ	Heat Affected Zone
SEM	Scanning Electron Microscope
σ_y	Yield strength
σ_0	Original yield strength
d	Average grain size
k	Hall-Petch constant

This paper has been updated. A corresponding Correction Notice has been published detailing the change.

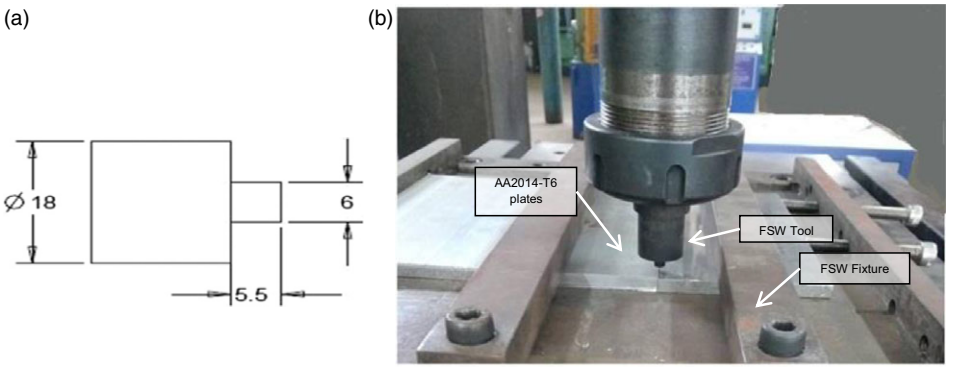

Figure 1. *FSW tool and fixture (all dimensions are in mm).*

1.0 Introduction

Friction stir welding (FSW) is a solid state welding process widely used for joining Aluminum alloys, because of its ability to produce defect-free joints, which is shown in Fig. 1. The joints produced by FSW have high tensile strength, improved hardness and low distortion compared to the conventional welding processes [1–6]. The aluminum alloy AA2014-T6, a copper-based aluminum alloy, is used predominantly in aeronautical, naval and automotive applications because of its superior mechanical properties. Many researchers have studied the effect of process parameters on the tensile strength and hardness characteristics of the aluminum alloy AA2014-T6 in the recent past [8–16].

Kadaganchi et al. [15] developed a regression model by employing the response surface methodology to optimise the process parameters of friction stir welded joints of AA2014-T6. It was observed that the developed model could predict the ultimate tensile strength and percentage elongation with less than 10% error. Ghetiya and Patel [16] developed a mathematical model to predict the tensile strength of immersed friction stir welds of AA2014-T4. It was reported that the developed model could predict the tensile strength with less than 3.23% error.

Babajanzade Roshan et al. [17] have employed an adaptive neuro-fuzzy inference system (ANFIS) and a simulated annealing algorithm to predict the tensile strength, yield strength and hardness. Using the developed model, they optimised the welding parameters. They have developed four different ANFIS models using four different membership functions (MFs) for input parameters. The model that yielded the least Root Mean Square Error (RMSE) value was chosen for the predictive model. It was observed that the generalised bell-type MF has resulted in the lowest RMSE of 6.64. Rahimzadeh Ilkhichi et al. [18] have developed a mathematical model using RSM to predict the hardness and grain size of FSW joints of aluminum alloy AA 7020. They have observed that the minimum value of grain size (10.9μm) and maximum amount of hardness (82HV) were obtained with the optimised rotational speed, traverse speed and axial force of 800rpm, 125mm/min, 8kN respectively. Vaira Vignesh et al. [19] have employed the ANFIS model for predicting the tensile shear failure load (TSFL) of friction stir spot welding (FSSW) joints of the aluminum alloy AA 6061. They have adopted the Box-Behenken design for conducting experiments.

Dewan et al. [20] have predicted the tensile strength of FSW joints of the aluminum alloy AA2219-T87 by adaptive neuro-fuzzy inference system (ANFIS) and an artificial neural network (ANN). Shanavas and Dhas [21] developed fuzzy logic model and regression model for the prediction of ultimate tensile strength and percentage elongation of friction stir weld joints of AA 5052 H32 aluminium alloy. They have developed a Mamdani-type fuzzy logic model and a regression model. It was observed that the regression model and the fuzzy logic model predicted the output function with a maximum error of 7% and 4% respectively.

There is much research being conducted on the prediction of mechanical characteristics like tensile strength and nugget hardness of friction stir welded aluminum alloys [15–24]. However, there are only

https://doi.org/10.1017/aer.2022.90 Published online by Cambridge University Press

Table 1. *The measured chemical composition of AA2014-T6 plates*

Element	Al	Cr	Cu	Mg	Mn	Si	Ti	Fe	Zn
Wt %	93.80	0.008	3.96	0.56	0.48	0.67	0.066	0.16	0.057

Table 2. *Friction stir welding process parameters*

	Process Parameters		
Levels	Tool rotational Speed (rpm) TRS	Welding speed (mm/min) WS	Axial force (kN) AF
1	700	20	10
2	1,000	35	12
3	1,400	50	14

a few works that developed efficient predictive models for FSW joints of the aluminum alloy AA2014-T6 for predicting mechanical characteristics. In the proposed research work, a Mamdani-type fuzzy logic-based model has been developed to predict the tensile strength and nugget hardness of friction stir welded joints of aluminum alloy AA2014-T6. The membership functions for input parameters and output responses are chosen as Gaussian and triangular membership functions respectively. The proposed model predicts the responses with an error of less than 2.5%.

2.0 Materials and methods

The plates of aluminum alloy AA2014-T6, cut to a size of 100mm × 50mm × 6mm were friction stir welded using an FSW machine. The FSW machine has a maximum spindle speed of 3,000rpm, a maximum welding speed of 200mm/min and can apply an axial load of up to 20kN. The chemical composition of the aluminum alloy plates was tested for spectrograph before being used in the experiments. It was found that the percentage of various elements present is well within the acceptable range. The measured chemical composition based on the spectrograph is shown in Table 1. Rajendran et al. [22] have investigated the effect of FSW parameters on the strength of AA2014-T6 aluminum alloy joints. The plates are of 2mm thickness. They have employed five levels for the welding parameters, namely tool rotational speed, welding speed, tool shoulder diameter and tool tilt angle. They have varied the tool rotational speed ranging from 1,300 to 1,700rpm, welding speed ranging from 20 to 60mm/min, tool shoulder diameter from 4 to 8mm and tool tilt angle from 0.5° to 2.5°.

Preliminary experiments were conducted with various process parameters at different levels. The specimens were subjected to ultrasonic Non-Destructive Testing (NDT). Ultrasonic test method of (NDT is being utilised for testing FSW joints. The ultrasonic test method is effective in determining most of the flaws in FSW joints like tunnel defects, warm holes and kissing bonds [25, 26]. It was observed from the tests that the specimens welded with tool rotational speeds of less than 700rpm and greater than 1,400rpm contain defects such as lack of penetration and wormhole respectively due to less plasticised material flow and high heat input respectively. The specimens welded with a welding speed greater than 50mm/min were observed to contain tunnel defect due to less plasticised material flow. Hence, the tool rotational speed was limited between 700 and 1,400rpm and the welding speed was limited between 20 and 50mm/min. In the current work, friction stir welding was carried out by varying tool rotational speed (TRS), welding speed (WS) and axial force (AF) at three levels. The welding process parameters and the levels are shown in Table 2. The tool was made of H13 tool steel. The tool used in the experimentation had a square cross section of side 6mm and length of the probe was 5.5mm. The tool had a shoulder diameter of 18mm. The dimensions of the tool and the fixture used are shown in Fig. 1. The tool tilt angle was kept constant at 2° throughout the experiment.

https://doi.org/10.1017/aer.2022.90 Published online by Cambridge University Press

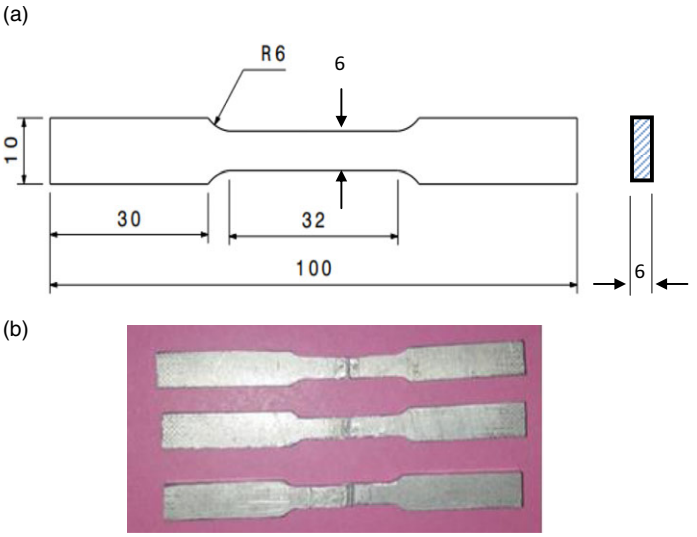

Figure 2. *(a) Dimensions of the tensile specimen in mm (b) Sample tensile specimen (after the test).*

The experiments were conducted as per Taguchi's L27 orthogonal array for the three process parameters at three levels. Mohamed MA et al. [23] have utilised the Taguchi L9 orthogonal array for predicting the mechanical properties and weld quality of FSW joints of the alloy AA6061-T651. They have varied rotational speed and traverse speed at three levels. They have employed the Multi-objective Taguchi Method (MTM) and Response Surface Methodology (RSM) for model development and optimisation. Wakchaure et al. [24] have utilised the Taguchi L27 orthogonal array for predicting the tensile strength of FSW joints of the alloy AA6082- T6. They have employed the Taguchi-based Grey Relational Analysis (GRA) and the Artificial Neural Network (ANN) for model development and optimisation.

The tensile specimens have been prepared in accordance to ASTM E8M-04 guidelines. The welded plates have been cut using power hacksaw and finished to the required dimension by machining. The tensile test was carried out using a 100kN, universal testing machine. The tensile specimens have been cut in such a way that the weld region is in the middle of the specimen. All tensile tests have been carried out perpendicular to the welding direction to determine the tensile properties of the welded joints. The specimen was subjected to load at a rate of 1.5kN/min. The tests were repeated three times, and the average values were taken for evaluation. The dimensions of the tensile specimen and sample tensile specimen after the test are shown in Fig. 2.

A Mitutoyo-make Vickers hardness tester was used to measure the hardness of the welded specimens. Hardness measurements across the transverse cross-section of the welded specimen were made with a load of 100g and a dwell time 30s.

The base metal was tested for tensile strength and hardness as per the procedure and standards stated above. Three samples were tested for each of the tests. The average values of tensile strength and the Vickers hardness number for the base metal are 461N/mm^2 and 155, respectively.

3.0 Development of fuzzy logic model

3.1 Fuzzy inference systems

There are two main types of fuzzy inference systems namely, (i) Mamdani-type and (ii) Sugeno-type. The main difference between the two types of FIS is how the output is generated from the fuzzy input. The defuzzification of a fuzzy output is done in the Mamdani-type FIS, whereas weighted average is used in the Sugeno-type FIS to compute the crisp output.

https://doi.org/10.1017/aer.2022.90 Published online by Cambridge University Press

Table 3. *Fuzzy variables, range of input parameters and responses*

	Input		
Parameters	Tool rotation speed (rpm) TRS	Welding speed (mm/min) WS	Axial force (mm) AF
Linguistic variables		L – Low M – Medium H – High	
Range	700 – 1,400	20–50	0.2–0.4
	Response		
Parameters	Tensile strength (N/mm^2) TS		Nugget hardness NH
Linguistic variables		L – Low M – Medium H – High	
Range	296–396		109–135

In the Mamdani-type fuzzy inference system, the output of each rule is a fuzzy set. The Mamdani-type systems are well suited to expert system applications as the rule bases used are comprehensible and highly instinctive.

In this work, a Mamdani-type fuzzy logic model was developed using the chosen input parameter range and output responses. The development of fuzzy logic model involves the following three steps:

Step 1. Fuzzification of variables

Step 2. Fuzzy inference process

Step 3. Defuzzification

In the fuzzification step, the input parameters and the output responses are coded into linguistic variables as Low, Medium and High. The linguistic variables, the range of input process parameters and output responses are shown in Table 3. In the second step membership functions are selected for input variables and output responses.

The membership functions can be of different types, such as triangular, trapezoidal, Gaussian, bell-shaped, sigmoidal and S-curve. The exact type to be used is selected based on the actual applications. In this work, Gaussian membership function was used for the input parameters because of the complex interactions between the input parameters and triangular membership function was used for the output parameters. The fuzzy logic model is shown in Fig. 3. The membership function plots for the input parameters and the output responses are shown in Fig. 4.

Defuzzification process was carried out using the centroid method. The fuzzy rule set used for simulating the model and the rule viewer are shown in Fig. 5.

4.0 Results and discussion

4.1 Experimental results

The experiments were conducted as per the Taguchi L_{27} full factorial design for the three welding parameters at three levels [24]. Each of the 27 experiments has been replicated three times, and the average values are taken for evaluation in order to eliminate the errors that might have been caused during the

https://doi.org/10.1017/aer.2022.90 Published online by Cambridge University Press

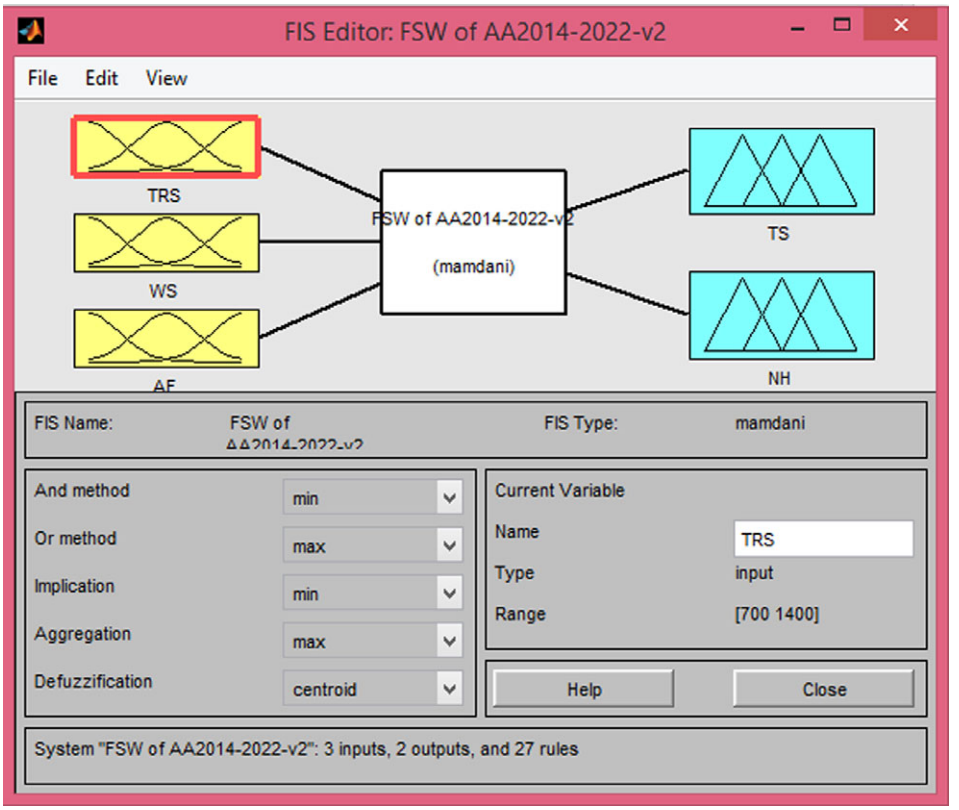

Figure 3. *Fuzzy logic model.*

experimentation. The average tensile strength and average Vickers hardness values as obtained from the experiments are shown in Table 4.

The hardness profiles of three sample specimen are shown in Fig. 6.

The hardness profile shows a "W" shape, which is unsymmetrical about the centreline of the weld. The hardness in the nugget region of the specimen is higher compared to the TMAZ and HAZ regions. It is also observed that the hardness values are slightly lower on the retreating side compared to the advancing side. The drop in the hardness value in the retreating side may be due to the stress that is incurred during the tool rotation and traverse as the direction of tool rotation is opposite to the tool movement in that side. It is also observed that the hardness values of the samples welded with low tool rotation speed (700rpm) is lower compared to the samples welded with 1,000 and 1,400rpm. It is also observed from the results that the nugget, HAZ and TMAZ regions have lower hardness compared to the base metal. This is due to the coarsening and or dissolution of strengthening precipitates during the weld thermal cycle.

The fracture surfaces of the tensile specimen are analysed by the SEM images of the fractured region. The SEM images of the fracture surfaces are shown in Fig. 7. It can be perceived from the images that there are dimples of various shapes and size on the fracture surfaces. The density of dimples is higher in samples welded with low tool rotation speed of 700rpm compared to the higher tool rotation speeds. This is evident from the Fig. 7(a) and (b). The larger density of dimples corresponds with the higher tensile strength of the joints. The enhanced strength of the joints is in accordance with the Hall-Petch relationship, which is given in Equation (1).

$$\sigma_y = \sigma_0 + kd^{-1/2} \tag{1}$$

https://doi.org/10.1017/aer.2022.90 Published online by Cambridge University Press

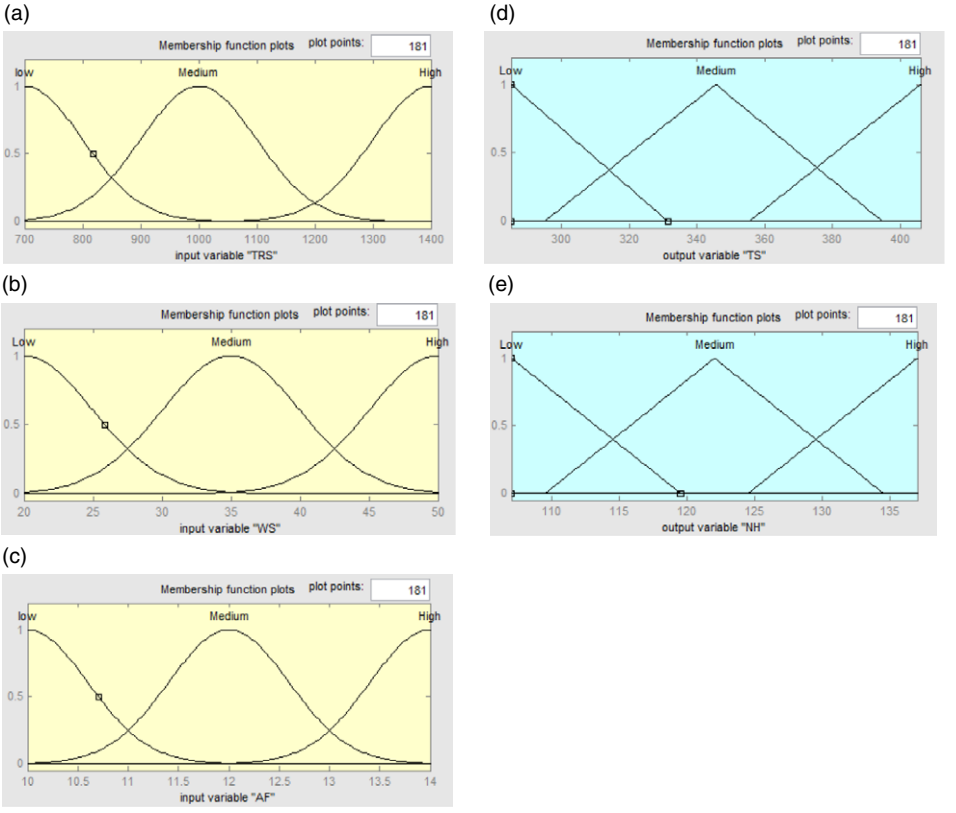

Figure 4. *Membership function plots (a) Tool rotation speed (b) Welding speed (c) Axial force (d) Tensile strength (e) Nugget hardness.*

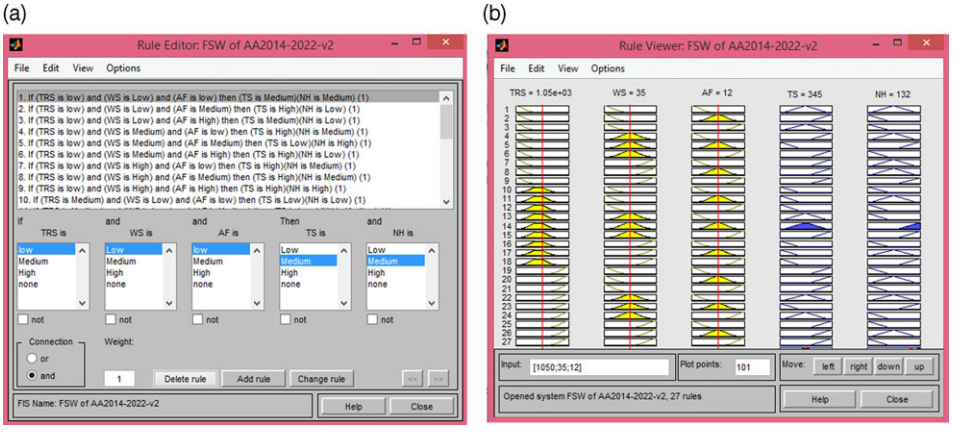

Figure 5. *(a) Fuzzy rules (b) Fuzzy rule viewer.*

https://doi.org/10.1017/aer.2022.90 Published online by Cambridge University Press

Table 4. *Experimental tensile strength and nugget hardness values*

Expt No	Tool rotation speed (rpm)	Welding speed (mm/min)	Axial force (kN)	Tensile Strength (N/mm^2)	Nugget hardness
1	700	20	10	339	124
2	700	20	12	382	114
3	700	20	14	350	110
4	700	35	10	385	124
5	700	35	12	298	130
6	700	35	14	382	111
7	700	50	10	394	124
8	700	50	12	396	120
9	700	50	14	384	134
10	1,000	20	10	298	114
11	1,000	20	12	339	124
12	1,000	20	14	297	113
13	1,000	35	10	341	110
14	1,000	35	12	352	132
15	1,000	35	14	338	135
16	1,000	50	10	296	114
17	1,000	50	12	308	124
18	1,000	50	14	304	130
19	1,400	20	10	392	111
20	1,400	20	12	395	123
21	1,400	20	14	386	113
22	1,400	35	10	342	120
23	1,400	35	12	308	132
24	1,400	35	14	339	109
25	1,400	50	10	381	113
26	1,400	50	12	394	123
27	1,400	50	14	384	110

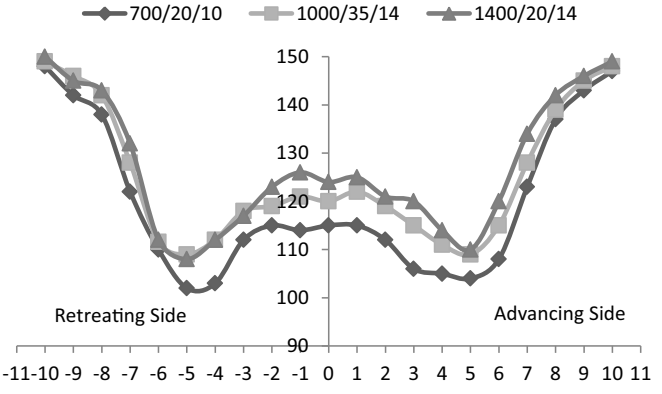

Figure 6. *Hardness profiles of sample specimen.*

https://doi.org/10.1017/aer.2022.90 Published online by Cambridge University Press

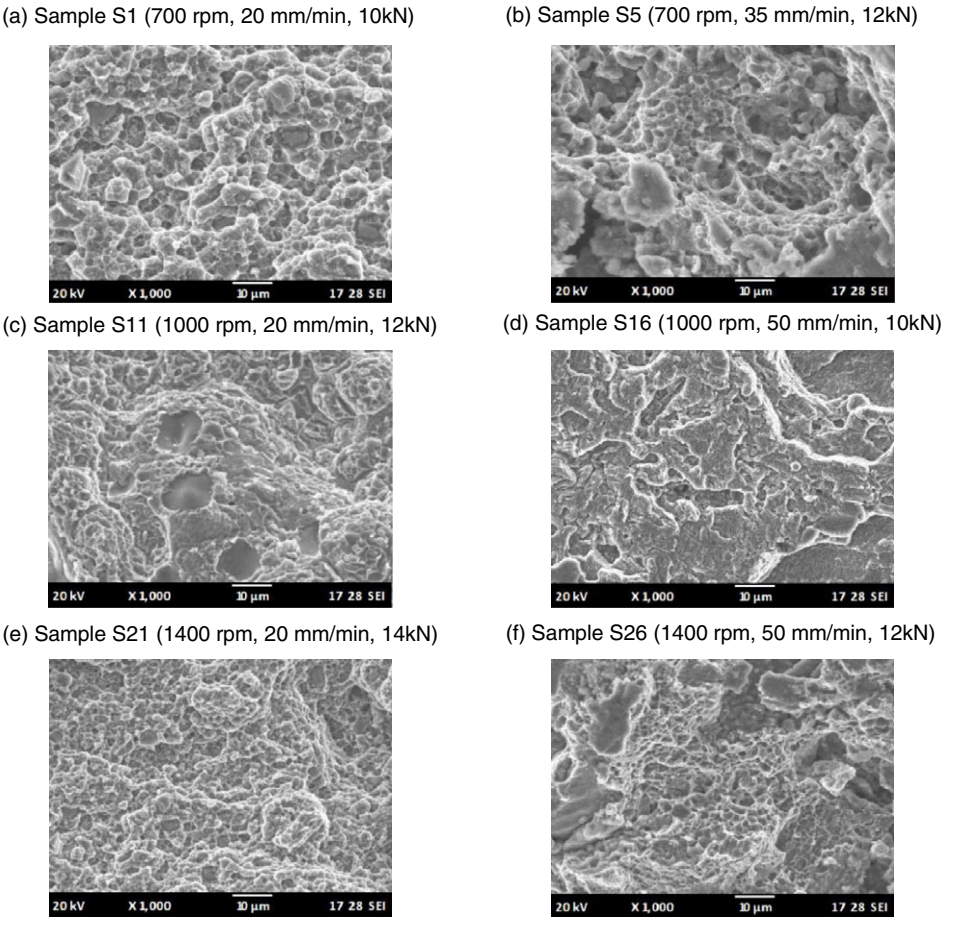

Figure 7. *SEM images of fractured surfaces of the tensile samples.*

According to this relationship, the yield strength (σ_y) of the material is inversely proportional to the square of the grain size (d). Hence, the strength of the material increases with the decrease in grain size [27]. The finer grain size is due to the large heat input attributed to the low tool rotation speeds.

The SEM images of the samples S11 and S16 are shown in Fig. 7(c) and (d). Fewer dimples with cleavage facets are seen in the fracture surfaces of the joints welded with 1,000rpm. The coarser dimples are attributed to plastic fracture. The coarser dimples are attributed to the low heat input during welding, which is caused by the higher tool rotation speed [18].

The increase in tool rotation speed has resulted in a combined mode of failure. It can be observed from Fig. 7(d) and (f) that there are finer dimples with cleavage facets in the microstructure of the sample S16 and S26, respectively. Deep holes and pluck out regions are observed on the microstructure of the joints welded with higher tool rotation speed.

4.2. Accuracy of the developed fuzzy model

Root Mean Square Error (RMSE) metrics has been used to find the accuracy of the developed model [17]. The RMSE can be calculated by the Equation (2)

$$RMSE = \sqrt{\frac{\sum_{i=1}^{N} (x_i - x'_i)^2}{N}} \tag{2}$$

https://doi.org/10.1017/aer.2022.90 Published online by Cambridge University Press

Table 5. *Results of confirmation experiments and results predicted by the model*

Exp No	Tool rotation speed (rpm)	Welding speed (mm/min)	Axial force (kN)	Tensile strength (N/mm^2)	Predicted tensile strength (N/mm^2)	Percentage deviation	Nugget hardness (HVN)	Predicted nugget hardness (HVN)	Percentage deviation
1	800	30	11	339	342	−0.88	128	126	1.56
2	800	40	13	382	376	1.57	132	129	2.27
3	900	30	11	350	348	0.57	120	122	−1.67
4	900	40	13	385	382	0.78	124	127	−2.42
5	1,100	30	11	298	302	−1.34	118	116	1.69
6	1,100	40	13	382	386	−1.05	122	120	1.64
7	1,200	30	11	394	387	1.78	124	126	−1.61
8	1,200	40	13	396	386	2.53	120	119	0.83
9	1,300	30	11	384	380	1.04	110	112	−1.82
10	1,300	40	13	298	305	−2.35	114	116	−1.75

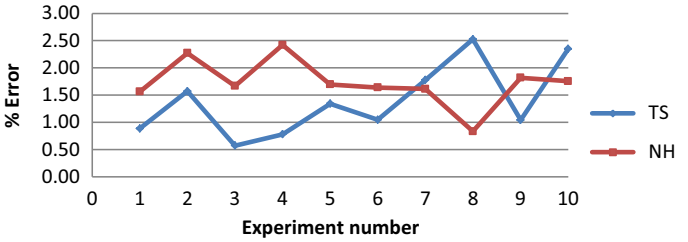

Figure 8. *% Error between the experimental and predicted values.*

where

i = variable
x_i = Actual observations
x'_i = Estimated values
N = Total data points

An RMSE was calculated between the experimental values and the values as obtained from the model. The calculated RMSE values for tensile strength and nugget hardness are 5.51and 2.16, respectively. The lower the value of the RMSE, the higher the accuracy of the model. The obtained values of RMSE are found to be lower and hence the accuracy of the model is higher.

4.3. Confirmation experiment results vs predicted results

To evaluate the fuzzy model, confirmation experiments were conducted by using ten new welding parameter values that are not used in the experiments used for developing the model. The values of the ten new welding parameters used for confirmation experiments are shown in Table 5.

The developed fuzzy logic model is validated by comparing the results of the confirmation experiments with that of the predicted values by the fuzzy model. The percentage of error between the experimental and predicted value is calculated using Equation (3)

$$\%\ Error = \frac{Experimental\ Value - Predicted\ Value}{Experimental\ Value} \times 100 \tag{3}$$

The variations between the results predicted by model and experimental values are shown in Fig. 8.

https://doi.org/10.1017/aer.2022.90 Published online by Cambridge University Press

(a) Variation of TS for WS and TRS

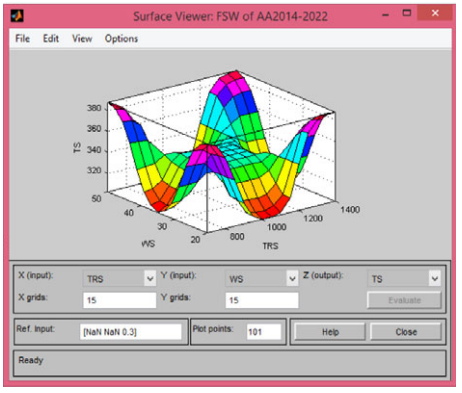

(b) Variation of NH for WS and TRS

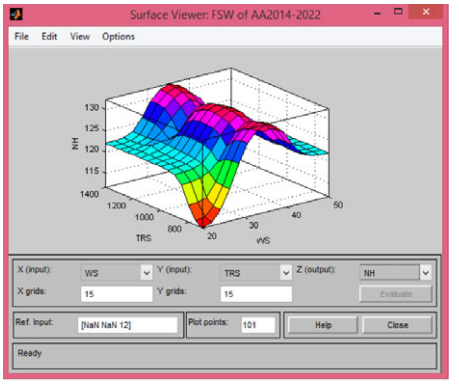

(c) Variation of TS for AF and TRS

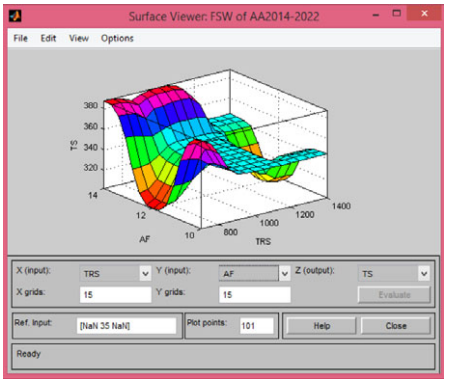

(d) Variation of NH for AF and TRS

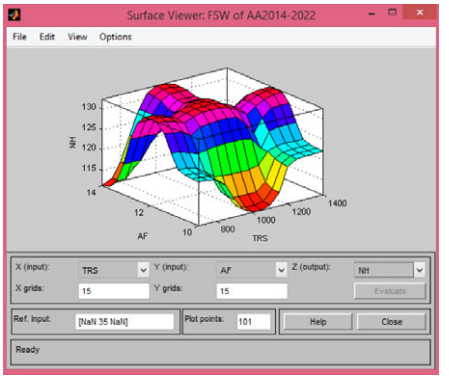

(e) Variation of TS for AF and WS

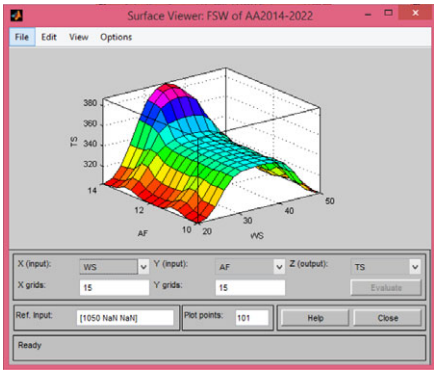

(f) Variation of NH for AF and WS

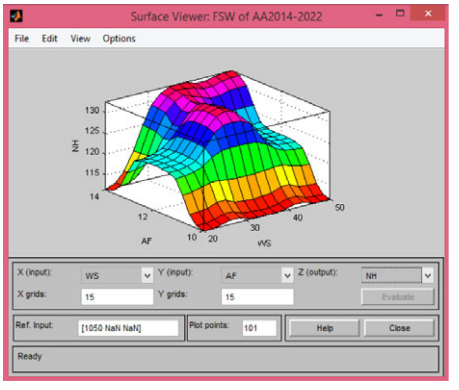

Figure 9. *Interaction of input parameters with output responses.*

It is inferred from the results that the % error between the experimental values and the predicted values are minimum. The maximum % error is 2.53% for tensile strength and 2.42% for weld nugget hardness.

The interaction of input parameters on the output responses is represented by surface plots. Figure 9(a), (c), and (e) represent the variation of tensile strength in response to the input parameters, TRS, WS and AF. High tensile strength is predicted when both WS and TRS are lower and when WS or TRS is higher in the test range. The variation of nugget hardness is represented in Fig. 9(b), (d) and

https://doi.org/10.1017/aer.2022.90 Published online by Cambridge University Press

(f). The decrease in TRS and AF has resulted in increased hardness. The increase in WS has resulted in increased hardness for lower values of TRS. The higher TRS, lower WS and higher AF, due to more heat generation during FSW, have resulted in grain coarsening and hence lower hardness [15].

5.0 Conclusion

The aluminum alloy AA2014-T6 was friction stir welded by varying the tool rotational speed (TRS), welding speed (WS) and axial force (AF) at three levels. The experiments were conducted as per the Taguchi L_{27} full factorial design. A Mamdani-type fuzzy logic model was developed using selected data ranges. The RMSE metric was used to test the accuracy of the developed model. It was found that the RMSE values for tensile strength and hardness are 5.51 and 2.16, respectively. The developed model was validated by comparing the values obtained from the confirmation experiment with the values predicted by the model. The calculated maximum error was 2.53% and 2.42% for tensile strength and nugget hardness, respectively. The proposed model has resulted in lesser error compared to the fuzzy logic model and the regression model developed by Shanavas et al. [21]. Rajendran et al. [22] have predicted the tensile strength of AA2014-T6 with a maximum error of 5%. The developed model can be used to predict the tensile strength and nugget hardness of FSW joints of the aluminum alloy AA 2014-T6 within the parameter ranges used in the model.

References

[1] Chauhan, A. and Kumar, S. An overview of optimization techniques used for friction stir welding process parameters, *Research J. Eng. Tech.* 2018, **9**, (1), pp 21–26.

[2] Ghorbanzade, T., Soltanipour, A., Dehghani, K. and Chabok, A. Microstructural evolutions and mechanical properties of friction stir welded AA2024-3, *Proc. Inst. Mech. Eng. L: J. Mater. Des. Appl.*, 2016, **230**, (1), pp 75–87.

[3] Hejazi, I. and Mirsalehi, S.E. Mechanical and metallurgical characterization of AA6061 friction stir welded joints using microhardness map, *Trans. Nonferrous Metals Soc. China,* 2016, **26**, (9), pp 2313–2319.

[4] Kannusamy, A.S. and Ramasamy, R. Effect of post weld heat treatment and welding parameters on mechanical and corrosion characteristics of friction stir welded aluminium alloy AA2014-T6, *Trans. Canadian Soc. Mech. Eng.*, 2018, **43**, (2), pp 230–236.

[5] Mehta, M., Reddy, G.M., Rao, A.V. and De, A. Numerical modeling of friction stir welding using the tools with polygonal pins, *Defence Technol.*, 2015, **11**, (3), pp 229–236.

[6] Franchim, A.S., Fernandez, F.F. and Travessa, D.N. Microstructural aspects and mechanical properties of friction stir welded AA2024-T3 aluminium alloy sheet, *Mater. Des.*, 2011, **32**, (10), pp 4684–4688.

[7] Sharma, C., Dwivedi, D.K. and Kumar, P. Effect of welding parameters on microstructure and mechanical properties of friction stir welded joints of AA7039 aluminum alloy, *Mater. Des.*, 2012, **36**, pp 379–390.

[8] Vagh, A. and Pandya, S. Influence of process parameters on the mechanical properties of friction stir welded AA 2014-T6 Alloy using Taguchi orthogonal array, *Int. J. Eng. Sci. Emerg. Technol.*, 2012, **2**, (1), pp 51–58.

[9] Tiwari, S.K., Shukla, D.K. and Chandra, R. Friction stir welding of aluminum alloys: A review, *Int. J. Mech. Aerosp. Ind. Mechatron. Manufact. Eng.*, 2013, **7**, (12), 2403–2408.

[10] Wakchaure, P.N., Borkar, B.R. and Tajane, R.S. Effect of tool geometry on mechanical properties of friction stir welding of aluminium alloy AA2014-T6, *Nat. J. Electron. Sci. Syst.*, 2014, **5**, (2).

[11] Rajamanickam, N. and Balusamy, V. Effects of process parameters on mechanical properties of friction stir welds using design of experiment, *Indian J. Eng. Mater. Sci.*, 2008, **15**, pp. 293–299.

[12] Srinivasan, P.B., Arora, K.S., Dietzel, W., Pandey, S. and Schaper, M.K. Characterisation of microstructure, mechanical properties and corrosion behaviour of an AA2219 friction stir weldment, *J. Alloys Compounds.* 2010, **492**, (1–2), pp 631–637.

[13] Arora, K.S., Pandey, S., Schaper, M. and Kumar, R. Effect of process parameters on friction stir welding of aluminum alloy 2219-T87, *Int. J. Adv. Manufact. Technol.*, 2010, **50**, (9–12), pp 941–952.

[14] Ugender, S., Kumar, A. and Reddy, A.S. Experimental investigation of tool geometry on mechanical properties of friction stir welding of AA 2014 aluminium alloy, *Proc. Mater. Sci.*, 2014, **5**, pp 824–831.

[15] Kadaganchi, R., Gankidi, M.R. and Gokhale, H. Optimization of process parameters of aluminum alloy AA 2014-T6 friction stir welds by response surface methodology, *Defence Technol.*, 2015, **11**, (3), pp 209–219.

[16] Ghetiya, N.D. and Patel, K.M. Prediction of tensile strength and microstructure characterization of immersed friction stir welding of aluminium alloy AA2014-T4, *Indian J. Eng. Mater. Sci.*, 2015, **22**, (2), pp 133–140.

https://doi.org/10.1017/aer.2022.90 Published online by Cambridge University Press

[17] Babajanzade Roshan, S., Behboodi Jooibari, M., Teimouri, R., Asgharzadeh-Ahmadi, G., Falahati-Naghibi, M. and Sohrabpoor, H. Optimization of friction stir welding process of AA7075 aluminum alloy to achieve desirable mechanical properties using ANFIS models and simulated annealing algorithm, *Int. J. Adv. Manufact. Technol.*, 2013, **69**, (5), pp 1803–1818.
[18] Rahimzadeh Ilkhichi, A., Soufi, R., Hussain, G., Vatankhah Barenji, R. and Heidarzadeh, A. Establishing mathematical models to predict grain size and hardness of the friction stir-welded AA 7020 aluminum alloy joints. *Metallur. Mater. Trans. B*, 2015, **46**, (1), pp 357–365.
[19] Vignesh, R.V., Padmanaban, R., Arivarasu, M., Karthick, K.P., Abirama Sundar, A. and Gokulachandran, J. Analysing the strength of friction stir spot welded joints of aluminium alloy by fuzzy logic, In *IOP Conference Series: Materials Science and Engineering*, vol. 149, no. 1, p. 012136. IOP Publishing, 2016.
[20] Dewan, M.W., Huggett, D.J., Warren Liao, T., Wahab, M.A. and Okeil, A.M. Prediction of tensile strength of friction stir weld joints with adaptive neuro-fuzzy inference system (ANFIS) and neural network, *Mater. Des.*, 2016, **92**, pp 288–299.
[21] Shanavas, S. and Dhas, J.E. Quality prediction of friction stir weld joints on AA 5052 H32 aluminium alloy using fuzzy logic technique, *Mater. Today: Proc.*, 2018, **5**, (5), pp 12124–12132.
[22] Rajendran, C., Srinivasan, K., Balasubramanian, V., Balaji, H. and Selvaraj, P. Identifying the combination of friction stir welding parameters to attain maximum strength of AA2014-T6 aluminum alloy joints, *Adv. Mater. Process. Technol.,* 2018, **4**, (1), pp 100–119.
[23] Mohamed, M.A., Manurung, Y.H. and Berhan, M.N. Model development for mechanical properties and weld quality class of friction stir welding using multi-objective Taguchi method and response surface methodology, *J. Mech. Sci. Technol.*, 2015, **29**, (6), pp 2323–2331.
[24] Wakchaure, K.N., Thakur, A.G., Gadakh, V. and Kumar, A. Multi-objective optimization of friction stir welding of aluminium alloy 6082-T6 Using hybrid Taguchi-Grey relation analysis-ANN method. *Mater. Today Proc.*, 2018, **5** (2), pp 7150–7159.
[25] Węglowski, M.S. and Sikora, S. Ultrasonic tests of FSW joints, *Biuletyn Instytutu Spawalnictwa*, 2017, **2017**, (4), pp 15–23.
[26] Adamus, K. and Lacki, P. Assessment of aluminum FSW joints using ultrasonic testing. *Arch. Metallur. Mater.*, 2017, **62**.
[27] Heidarzadeh, A., Testik, Ö.M., Güleryüz, G. and Barenji, R.V. Development of a fuzzy logic based model to elucidate the effect of FSW parameters on the ultimate tensile strength and elongation of pure copper joints, *J. Manufact. Processes.* 2020, **53**, 250–259.

Cite this article: Ashok S.K. and Ponni alias sathya S. (2023). A fuzzy model to predict the mechanical characteristics of friction stir welded joints of aluminum alloy AA2014-T6. *The Aeronautical Journal*, **127**, 818–830. https://doi.org/10.1017/aer.2022.90